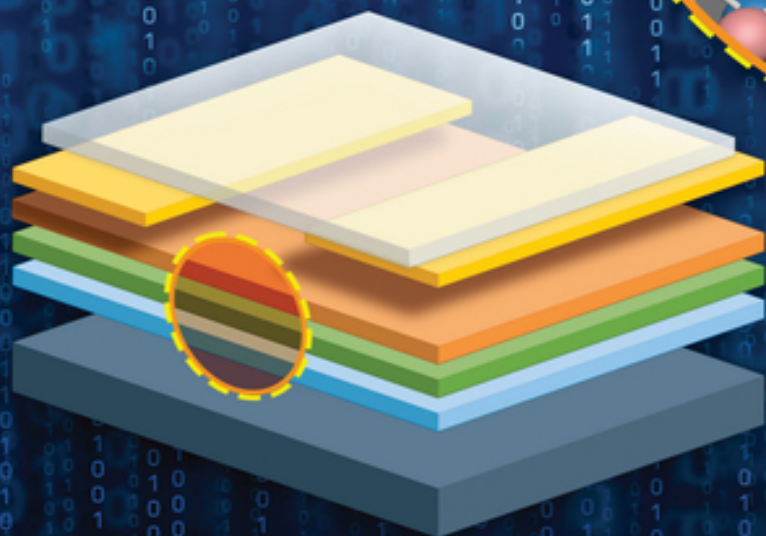
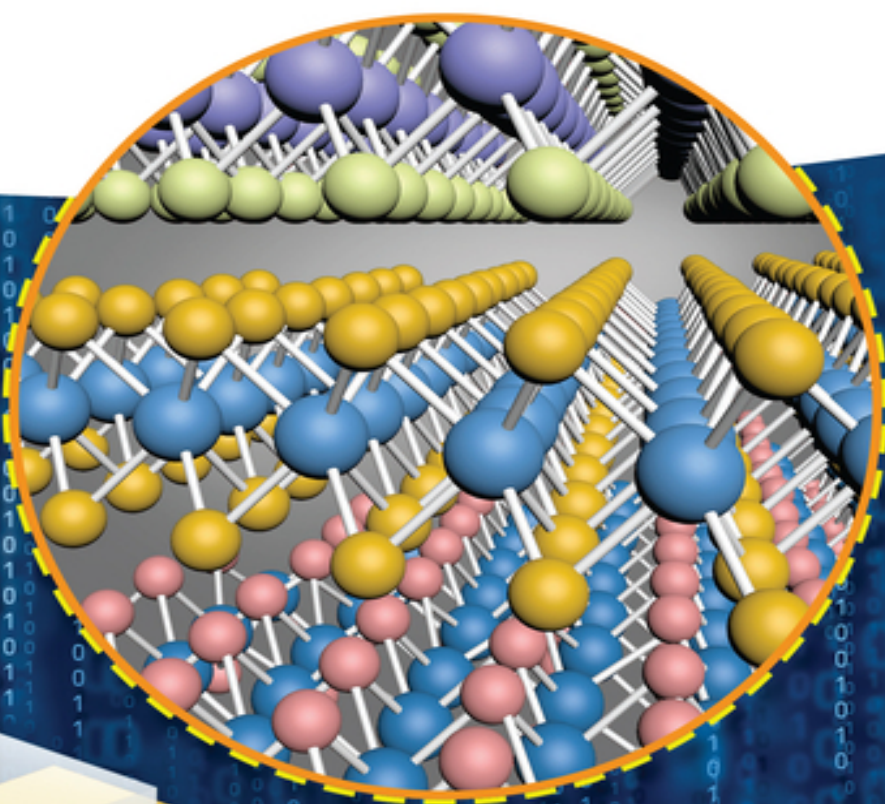


Edited by Zheng Zhang, Zhou Kang,  
Qingliang Liao, and Yue Zhang

# Van der Waals Heterostructures

Fabrications, Properties, and Applications



# Table of Contents

[Cover](#)

[Title Page](#)

[Copyright](#)

[Preface](#)

[1 The 2D Semiconductor Library](#)

[1.1 Introduction](#)

[1.2 Emerging 2DLMs for Future Electronics](#)

[References](#)

[2 The 2D Semiconductor Synthesis and Performances](#)

[2.1 Exfoliation](#)

[2.2 Chemical Vapor Deposition](#)

[References](#)

[3 The VdW Heterostructure Controllable Fabrications](#)

[3.1 Wet Transfer](#)

[3.2 Controllable Selective Synthesis](#)

[3.3 Dry Transfer](#)

[References](#)

[4 The Mixed-dimensional VdW Heterostructures](#)

[4.1 Categorization of Mixed-dimensional VdWHs](#)

[4.2 Strategies for Constructing Mixed-dimensional VdWHs](#)

[4.3 Electronic and Sensing Applications](#)

[4.4 Optoelectronic and Photonic Applications](#)

[4.5 Energy Applications](#)

[4.6 Conclusions](#)

[References](#)

## 5 The VdW Heterostructure Interface Physics

5.1 Band Alignment and Charge Transfer in VdWHs

5.2 Magnetic Coupling in VdWHs

5.3 Moiré Pattern

5.4 VdWHs for Protection

5.5 Characterization Techniques for VdWHs

References

## 6 The VdW Heterostructure Multi-field Coupling Effects

6.1 Introduction

6.2 The Multifield Coupling Effect Characterization for 2D Van der Waals Structures

6.3 The Multifield Modulation for Electrical Properties of 2D Van der Waals Structures

6.4 The Multifield Modulation for Optical Properties of 2D Van der Waals Structures

References

## 7 VdW Heterostructure Electronics

7.1 Van der Waals PN Junctions

7.2 Van der Waals Metal-Semiconductor Junctions

7.3 Field-effect Transistor

7.4 Junction Field-Effect Transistor

7.5 Tunneling Field-Effect Transistor

7.6 Van der Waals Integration

References

## 8 VdW Heterostructure Optoelectronics

8.1 Photodetectors

8.2 Light Emission

8.3 Optical Modulators

References

## [9 VdW Heterostructure Electrochemical Applications](#)

[9.1 Solar Energy](#)

[9.2 Van der Waals Heterostructure Application in Hydrogen Energy](#)

[9.3 Battery](#)

[9.4 Catalyst](#)

[9.5 Biotechnology](#)

[References](#)

## [10 Perspective and Outlook](#)

[10.1 Overall Development Status of 2D Materials](#)

[10.2 Compatibility Between 2D Van der Waals Device Processing and Silicon Technology](#)

[10.3 Promising Roadmap of Van der Waals Heterostructure Devices \[Medium term: 5 years, Long term: 5-10 years\]](#)

[10.4 Promising Roadmap of Optoelectronic Device](#)

[10.5 Conclusion and Prospect](#)

[References](#)

[Index](#)

[End User License Agreement](#)

## **List of Tables**

Chapter 8

[Table 8.1 Summary of vdWH photodetectors \(Gr: graphene; GO: graphene oxide;...](#)

[Table 8.2 Summary of typical VdWH LEDs \(Gr: graphene; BP: black phosphorus;...](#)

## **List of Illustrations**

## Chapter 1

[Figure 1.1 Two-dimensional materials for future electronic devices: from cel...](#)

[Figure 1.2 Brief introduction of graphene. \(a\) Relationship between conducta...](#)

[Figure 1.3 Structure and optoelectronic applications of graphite-acetylene g...](#)

[Figure 1.4 \(a\) Crystal structures of h-BN.](#)

[Figure 1.5 \(a\) 2H, 1T, 1T' structures schematic diagram of layer TMDCs...](#)

[Figure 1.6 Compositions of MXenes and MAX phases in periodic tables. \(a\) Ele...](#)

[Figure 1.7 \(a\) Crystal structures of MoO<sub>3</sub>; \(b\) crystal structures of V<sub>2</sub>O<sub>5</sub>; \(...](#)

## Chapter 2

[Figure 2.1 Exfoliated graphene films.](#)

[Figure 2.2 Exfoliation and characterization of large-area MoS<sub>2</sub> on Au substra...](#)

[Figure 2.3 Schematic illustration of the photo-induced exfoliation of MoS<sub>2</sub> i...](#)

[Figure 2.4 \(a\) Schematic diagram of WS<sub>2</sub>-growth and the effect of regulating ...](#)

[Figure 2.5 \(a\) Schematic image of LPCVD two-step synthesis of WSe<sub>2</sub>/SnS<sub>2</sub> vert...](#)

[Figure 2.6 \(a\) Schematic of experimental setup for PECVD including gaseous s...](#)

[Figure 2.7 \(a\) Atomic geometry of interface showing only the topmost graphen...](#)

## Chapter 3

[Figure 3.1 Simple schematic diagram of graphene film transfer by metal etchi...](#)

[Figure 3.2 The schematic diagram of the CVD-grown WS<sub>2</sub> film transferred on ta...](#)

[Figure 3.3 Illustration and live view of the transfer process of graphene fi...](#)

[Figure 3.4 Schematic diagrams of the high-fidelity wedging transfer process ...](#)

[Figure 3.5 Vertical 2D-2D van der Waals heterostructures. \(a\) Scanning trans...](#)

[Figure 3.6 Lateral 2D-2D heterostructures. Schematic illustration of the pre...](#)

[Figure 3.7 One-dimensional 2D-2D van der Waals heterostructures. \(a\) Schemat...](#)

[Figure 3.8 Controllable synthesis of 2D-1D heterostructures. \(a\) Growth and ...](#)

[Figure 3.9 Controllable synthesis of 2D-3D heterostructures. Schematics and ...](#)

[Figure 3.10 The scheme of transfer processes utilizes thermal-release tape. ...](#)

[Figure 3.11 Schematic process flow for the pick-up and drop-down process to ...](#)

[Figure 3.12 The computer-assisted design schematics, functionalities, and ph...](#)

## Chapter 4

[Figure 4.1 \(a\) Schematic of the dimensionality-dependent density of states a...](#)

[Figure 4.2 \(a\) Schematic of the typical transfer-assisted fabrication proces...](#)

[Figure 4.3 Electronic and chemical sensing applications of mixed-dimensional...](#)

[Figure 4.4 Optoelectronics based on 2D-1D mixed-dimensional vdWHs. \(a\) Optic...](#)

[Figure 4.5 Optoelectronics based on the 2D-3D mixed-dimensional vdWHs. \(a\) S...](#)

[Figure 4.6 Energy applications of mixed-dimensional hybrids. \(a\) 2D WS<sub>2</sub>/1D C...](#)

## Chapter 5

[Figure 5.1 \(a, b\) Schematics and results of the pump-probe configuration use...](#)

[Figure 5.2 \(a-c\) Stacking tunable interlayer magnetism of CrI<sub>3</sub>. Crystal. \(a\)...](#)

[Figure 5.3 \(a-c\) IQHE and FQHE in BP-h-BN vdWH.](#)

[Figure 5.4 \(a\) DAADF characterization of MoS<sub>2</sub>/WSe<sub>2</sub> vdWHs showing moiré patte...](#)

[Figure 5.5 \(a\) STS data measured on MoS<sub>2</sub>, WS<sub>2</sub>, and MoS<sub>2</sub>/WS<sub>2</sub> vdWHs.](#)

[Figure 5.6 \(a\) Two-dimensional PL mapping and the corresponding PL intensity...](#)

## Chapter 6

[Figure 6.1 The multifield microscopy techniques on 2D vdW structures. \(a\)Top...](#)

[Figure 6.2 The multifield optical spectroscopy techniques on 2D vdW structur...](#)

[Figure 6.3 Strain-engineered electrical properties of 2D vdW structures. \(a\)...](#)

[Figure 6.4 Strain-regulated optical properties of 2D vdW structures. \(a\) Sch...](#)

[Figure 6.5 Electric- and thermal-engineered optical properties for 2D vdW st...](#)

## Chapter 7

[Figure 7.1 \(a\) Large-range  \$I\_{ds}\$  versus  \$V\_{ds}\$  curve of the device. Inset is the ...](#)

[Figure 7.2 \(a\) Structure schematic of the BP/ReS<sub>2</sub>-based TCAM cell and the eq...](#)

[Figure 7.3 \(a-f\) Fabrication processes of WSe<sub>2</sub> transistors using vdW integra...](#)

[Figure 7.4 \(a\) Schematic diagram of the simple structure of FET. \(b\) Schemat...](#)

[Figure 7.5 \(a\) The effective channel  \$b\$  of the JFET depletion layer width  \$W\_D\$ ...](#)

[Figure 7.6 \(a\) The fabrication process of SnSe/MoS<sub>2</sub> JFET. \(b\) Transfer chara...](#)

[Figure 7.7 \(a\) \(i\) Schematic diagram of the cross-section of n-type TFET, \(i...](#)

[Figure 7.8 \(a\) Photograph of a 2-in. MoS<sub>2</sub> wafer with 1-bit full-adder arrays...](#)

## Chapter 8

[Figure 8.1 \(a\) Schematic drawing of a p-MoTe<sub>2</sub>/n-MoS<sub>2</sub> vdWH for light sensing ...](#)

[Figure 8.2 \(a\) The measurement system for polarization-sensitive photodetect...](#)



[Figure 8.3 \(a\) The BP-on-WSe<sub>2</sub> photodetector, \(b\) photocurrent microscopy ima...](#)

[Figure 8.4 \(a\) The fabricated BP/SnSe<sub>2</sub> heterojunction; \(b\) band alignment at...](#)

[Figure 8.5 \(a\) Band alignment of the photo-thermionic \(PTI\) effect at the Gr...](#)

[Figure 8.6 \(a\) 3D sketch of a top-gated WS<sub>2</sub> phototransistor. \(b\) Photorespon...](#)

[Figure 8.7 \(a\) The layout of a p-g-n heterostructure; \(b\) broadband photores...](#)

[Figure 8.8 \(a\) A cross-section view of the WSe<sub>2</sub>/MoS<sub>2</sub> diode; \(b\) the correspo...](#)

[Figure 8.9 \(a\) The cross-sectional view of the asymmetric LED. \(b\) EL from t...](#)

[Figure 8.10 \(a\) Schematic drawing of the n-MoS<sub>2</sub>/p-MoS<sub>2</sub>/p-GaN heterostructure...](#)

[Figure 8.11 \(a\) VdWH \(monolayer Gr/10-layer MoS<sub>2</sub>\) set on a flat mirror subst...](#)

[Figure 8.12 \(a\) Schematic drawing and \(b\) optical image of a vertical hetero...](#)

[Figure 8.13 \(a\) Schematic drawing of the Gr/MoS<sub>2</sub> modulator.](#)

[Figure 8.14 \(a\) Schematic sketch of the Gr/BN vdWH integrated with a silicon...](#)

## Chapter 9

[Figure 9.1 \(a\) Conversion of solar photons into three forms of energy in nat...](#)

[Figure 9.2 Van der Waals heterostructure for hydrogen production by water ph...](#)

[Figure 9.3 Van der Waals heterostructure for hydrogen production by water el...](#)

[Figure 9.4 \(a\) The discharge and charge mechanism of a LIB using heterostruc...](#)

[Figure 9.5 \(a-c\) Morphology engineering for 2D TMDC-based catalysts. The mod...](#)

[Figure 9.6 Vacancy and interface engineering for 2D TMDC-based catalysts. \(a...](#)

[Figure 9.7 \(a\) Research trends in 2D nanomaterials and some promising biomed...](#)

## Chapter 10

[Figure 10.1 The nondestructive optical techniques for revealing the layer-re...](#)

[Figure 10.2 Compatibility and difference between 2D materials and traditiona...](#)

[Figure 10.3 Future integration paradigm based on van der Waals device.](#)

[Figure 10.4 2D van der Waals optoelectronic device development.](#)

# **Van der Waals Heterostructures**

## **Fabrications, Properties, and Applications**

*Edited by Zheng Zhang, Zhuo Kang, Qingliang Liao,  
and Yue Zhang*

## **Editors**

### ***Dr. Zheng Zhang***

University of Science & Technology Beijing  
Department of Materials  
Physics & Chemistry  
Xueyuan Road 30#  
Haidian District  
100083 Beijing  
China

### ***Dr. Zhuo Kang***

University of Science & Technology Beijing  
School of Materials Science and Engineering  
Xueyuan Road 30#  
Haidian District  
100083 Beijing  
China

### ***Dr. Qingliang Liao***

University of Science & Technology Beijing  
School of Materials Science and Engineering  
Xueyuan Road 30#  
Haidian District  
100083 Beijing  
China

### ***Dr. Yue Zhang***

University of Science & Technology Beijing  
Department of Materials  
Physics & Chemistry  
Xueyuan Road 30#  
Haidian District  
100083 Beijing  
China

**Cover:** FORMGEBER Mannheim

All books published by **WILEY-VCH** are carefully produced. Nevertheless, authors, editors, and publisher do not warrant the information contained in these books, including this book, to be free of errors. Readers are advised to keep in mind that statements, data, illustrations, procedural details or other items may inadvertently be inaccurate.

**Library of Congress Card No.:** applied for

**British Library Cataloguing-in-Publication Data:**

A catalogue record for this book is available from the British Library.

**Bibliographic information published by the Deutsche Nationalbibliothek**

The Deutsche Nationalbibliothek lists this publication in the Deutsche Nationalbibliografie; detailed bibliographic data are available on the Internet at <http://dnb.d-nb.de>.

© 2023 Wiley-VCH GmbH, Boschstraße 12, 69469 Weinheim, Germany

All rights reserved (including those of translation into other languages). No part of this book may be reproduced in any form – by photoprinting, microfilm, or any other means – nor transmitted or translated into a machine language without written permission from the publishers. Registered names, trademarks, etc. used in this book, even when not specifically marked as such, are not to be considered unprotected by law.

**Print ISBN** 978-3-527-34950-0

**ePDF ISBN** 978-3-527-83386-3

**ePub ISBN** 978-3-527-83387-0

**oBook ISBN** 978-3-527-83388-7

# Preface

As the feature size of semiconductor devices keeps shrinking along Moore's law, the principle that has powered the information technology revolution since the 1960s, the physical limits to silicon-based transistors have been reached, resulting in severe performance degradations caused by short-channel effects, gate oxide tunneling, and surge in power consumption. In order to further downscale the transistors without performance degradations in the post-Moore era, massive research has been carried out to explore revolutionary new materials and devices. Among them, two-dimensional (2D) layered materials, including graphene, transition metal dichalcogenides (TMDCs), and related van der Waals (vdW) structures, have been proven to possess great potential for future post-Moore electronics, optoelectronics, etc.

2D materials possess unique properties with covalently bonded in-plane and dangling-bond free surfaces, which ensure monolayers can be stacked on top of each other and held together by interlayer vdW forces. Besides, 2D materials can be integrated into a new type of heterostructures with other materials in various dimensions, including zero-dimensional (0D) nanoparticles, one-dimensional (1D) nanowires, 2D films, and three-dimensional (3D) bulk materials, by exceeding the limitation of close lattice match at the interface. Except for 2D-2D heterostructures, other structures are so-called mixed-dimensional vdW heterostructures. In these heterostructures, the weak vdW forces between the neighboring materials make each material maintain its original electronic structure, without the influence of the interface structure variations. The convenience of this

combination leads to many new phenomena, devices, and mechanisms, such as the 0D-2D photo gating effect, static electrical doping, and 1D-2D nanowire gating. The underlying physics phenomena and possible applications in integrated circuits, sensors, or energy harvesting have attracted broad interest in academia and industry. In a word, vdW heterostructures provide the promising opportunity to combine different materials with unique properties as the building blocks of engineering new functional structures for the fabrication and applications of 2D electronic and optoelectronic devices.

Our group has been devoted into TMDCs semiconductors and their 0D-2D, 1D-2D, 2D-2D, and 2D-3D vdW heterostructures since 2013. Recently, along with the highly developed multi-disciplinary integration, considerable progress has been achieved in fundamental research and technological applications of TMDCs vdW heterostructures. This book covers state-of-the-art theoretical and experimental research on vdW heterostructures and their applications as electronic and optoelectronic devices. This book is divided into 10 chapters and guided by Dr. Zheng Zhang, Dr. Yue Zhang, Dr. Zhuo Kang, and Dr. Qingliang Liao. The detailed chapter theme and authors are as follows: [Chapter 1](#), “The 2D semiconductor library” (Zheng Zhang and Yue Zhang); [Chapter 2](#), “The 2D semiconductor synthesis and performances” (Xiang Chen, Qijie Liang, and Yue Zhang); [Chapter 3](#), “The vdW heterostructure controllable fabrications” (Zheng Zhang, Qingliang Liao, and Yue Zhang); [Chapter 4](#), “The mixed-dimensional vdW heterostructures” (Pei Lin, Baishan Liu, and Zheng Zhang); [Chapter 5](#), “The vdW heterostructure interface physics” (Guangjie Zhang, Yang Ou, Peifeng Li and Qingliang Liao); [Chapter 6](#), “The vdW heterostructure multi-field coupling effects” (Junli Du, Baishan Liu, and Zheng Zhang); [Chapter](#)

[7](#), “VdW heterostructure electronics” (Xiankun Zhang, Xiang Chen, and Yue Zhang); [Chapter 8](#), “VdW heterostructure optoelectronics” (Qi Zhang, Zhuo Kang, and Yue Zhang); [Chapter 9](#), “VdW heterostructure electrochemical applications” (Xiankun Zhang and Zhuo Kang); [Chapter 10](#), “Perspective and outlook” (Zheng Zhang and Yue Zhang). In addition to the help of the aforementioned members, the completion of the book is also inseparable from the unremitting efforts of the following doctoral students, including Huihui Yu, Li Gao, Wenhui Tang, Xiaofu Wei, Mengyu Hong, Ruishan Li, Yihe Liu, He Jiang, Kuanglei Chen, Haoran Zeng, Yanzhe Zhang, and Xuan Yu. With this book, I wish to thank my current and former group members, as well as the outstanding colleagues and collaborators who have dedicated themselves to this crucial research area.

The University of Science and Technology Beijing and the funding agencies also have my appreciation for providing the necessary support of the research work. Among the latter, special thanks are due to the National Natural Science Foundation of China (Nos. 51991340, 51991342, 92163205, 51972022), the National Key R&D Program of China (No. 2018YFA0703503), the Overseas Expertise Introduction Projects for Discipline Innovation (No. B14003), and the Natural Science Foundation of Beijing Municipality (Grant No. Z180011).

I worked consistently to accomplish this work with Wiley publisher. I hope that this contribution would further enhance the applied material sciences, especially in bringing new entrants into the nanotechnology fields, and help scientists to come forward and develop their own field of specialization.

Last, but by no means least, I am deeply appreciative of the understanding and support shown by my family members,



without whom these achievements could never be obtained.

Dr. Yue Zhang  
Academician of Chinese Academy of Sciences  
Fellow of Royal Society Chemistry  
Editor-in-chief of National Science Open  
Engineering and Materials Science Associate Editor of  
Fundamental Research  
E-mail: [yuezhang@ustb.edu.cn](mailto:yuezhang@ustb.edu.cn)

# 1

## The 2D Semiconductor Library

Zheng Zhang<sup>1,2</sup>, and Yue Zhang<sup>1,2</sup>

<sup>1</sup> Academy for Advanced Interdisciplinary Science and Technology, Beijing Advanced Innovation Center for Materials Genome Engineering, University of Science and Technology Beijing, Beijing, China

<sup>2</sup> Beijing Key Laboratory for Advanced Energy Materials and Technologies, School of Materials Science and Engineering, University of Science and Technology Beijing, Beijing, China

### 1.1 Introduction

Since graphene mechanically stripped out in 2004, two-dimensional-layered materials (2DLMs) have received widespread concern due to the intrinsic changes of the physical and chemical characteristics caused by quantum confinement effect, which pertains to the nanoscale thickness [[1](#), [2](#)]. Since the carrier transport will be strongly restricted to the two-dimensional plane, the electronic and optoelectronic characteristics of the 2DLMs will change significantly [[3](#), [4](#)]. The 2D material family covers various components including most of the elements in the periodic [table](#) [[5](#)]. These 2D nanosheets usually have a well-defined crystal structure without surface dangling bonds, which has traditionally plagued most semiconductor nanostructures, and therefore exhibits superior electronic properties that are not easily available in other semiconductor nanostructures. This results in a wealth of electronic properties, as well as direct and indirect

bandgaps with visible light ranges from ultraviolet to infrared [6–8]. What is more, due to the excellent adaptability of 2D geometry to the existing process techniques in the semiconductor industry, 2DLMs are able to be integrated with conventional semiconducting materials such as silicon and are able to be transferred on diverse supporting substrates. As a result, it is of great potential for them in future applications such as nanoelectronics, optoelectronics, and new ultrathin flexible devices [6–18]. Two-dimensional atomic crystal integrated circuit has been demonstrated, including memory, logic gates, amplifiers, oscillators, mixers, switches, and modulators. Two-dimensional materials of only one or a few atoms thick hold the potential to make future optoelectronics and electronic devices. The functional integrated circuits (IC) of 2DLMs helps solve the technical and fundamental problems of the electronics industry.

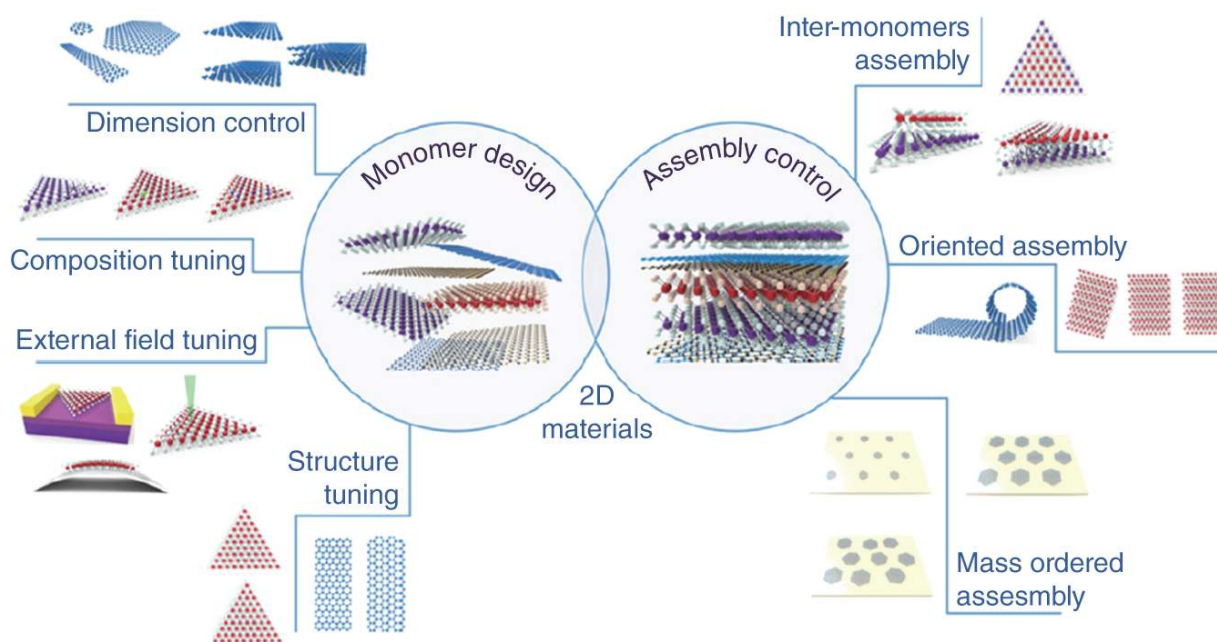


**Figure 1.1** Two-dimensional materials for future electronic devices: from cell unit to small integration.

*Source:* Reproduced with permission from Ref. [19], © American Chemical Society 2018.

The emerging application of nanoelectronics using two-dimensional materials prerequisites a reliable preparation and controlled stacking of wafer-scale 2DLMs of high quality by taking full advantage of their unique features in the two-dimensional limit ([Figure 1.1](#)). The widespread use of 2DLMs is due to their inherent properties and, to a large extent, their adjustability. Because of the novel anisotropy and planar crystal structure of 2DLMs, their properties can be improved greatly by adjusting the composition, size, field, and structure [[20](#)]. For instance, the band structure of a two-dimensional material changes significantly as the material thickness decreases from block to single-layer limit. In addition, some two-dimensional materials can be converted from semiconductor to metal through the intercalation. The use of one material in modern technology and applications is difficult to achieve a variety of excellent performance. As a result, 2DLMs can adjust their properties to the desired functionality, opening the way for further widespread use in electronic circuits.

Furthermore, since only one or a few atoms thick, 2DLMs with different heights can be stacked to form various heterostructures without consideration of lattice matching and processing compatibility. Van der Waals (vdW) heterostructures with sharp interfaces and disparate electronic properties offer a novel platform and prosperous applications for investigation of the creation, confining, and transmission of charge, excitons, and photons at two-dimensional limit [[18](#)]. The structure of a single two-dimensional material is also worth further study because it helps to further discover the intrinsic properties of the 2DLMs. New applications can be made by extending the structural deformation derived from directional construction to the properties of 2DLMs. In addition, efficient construction techniques are disposable to the production of large-scale nanodevices with desired-ordered

structures to address the scaling and integration challenges of microelectronics, photonics, and microelectromechanical systems [[21-24](#)].

## **1.2 Emerging 2DLMs for Future Electronics**

The rise of graphene with excellent properties has facilitated the discovery and research of new two-dimensional materials. In addition to graphene, various two-dimensional materials are attracting focus because of their unique properties. The size effect and adjustability of its energy band structure result in some novel properties. In this section, we will look at two aspects of the emerging 2DLMs. In one part, we will give clues based on the structure of two-dimensional materials, and in the other part, we will detail the various 2DLMs that are classified by their elemental composition.

### **1.2.1 Classification**

Initially, 2DLMs represented by graphene were referred to as a layered material that has strong intralayer covalent bonds and weak interlayer vdW coupling. Therefore, the layered material can be obtained by stripping the bulk material. In this case, we call them two-dimensional layered materials (2DLMs).

Lamellar vdW materials, which are separated into single or several layers, are one of the hot research topics. Due to the strong covalent bonds in planes and weak interlayer vdW coupling, they can be separated by mechanical or liquid stripping to form nanosheets [[8](#), [25](#)]. In addition to graphene, which was first discovered, transition metal dichalcogenide (TMDCs) are also typical vdW materials, such as  $\text{MoS}_2$ ,  $\text{WS}_2$ , and  $\text{WSe}_2$ . To date, more than 40 types

of TMDCs have been discovered [26]. Hexagonal boron nitride (h-BN) [27], silicon carbide [28], VO<sub>2</sub> [29], and telluride antimony [30] are also included within such category.

## 1.2.2 Elemental 2DMLs

2DMLs such as III-VA group and transition group are of great interest. Because of their unique ultrathin two-dimensional limit, they exhibit superior electronic, photonic, magnetic, and catalytic properties than bulk materials. These materials are of great potential for diverse applications in field effect transistors (FET), optoelectronics, memories, and artificial synapsis [31].

### 1.2.2.1 IV A Group

Since its discovery in 2004, graphene with the feature of honeycomb structure has been attracting great attention [2]. A range of methods for preparing graphene, such as mechanical stripping, liquid-assisted stripping, and chemical vapor deposition (CVD) methods, have rushed out. It has lots of superior properties, in particular its unprecedented high intrinsic mobility of  $200\,000\text{ cm}^2\text{ V}^{-1}\text{ s}^{-1}$  at room temperature [32]. Stampfer et al. discovered that it has the mobility at low temperature of  $350\,000\text{ cm}^2\text{ V}^{-1}\text{ s}^{-1}$ , as shown in [Figure 1.2a](#), reaching the highest record so far [35]. The grooves are utilized to suspend graphene. The beam of laser is concentrated on graphene, after which the heat flows radially from the graphene center to the peripheral. The dependence of Raman G peak on excitation power is measured, and the TC of graphene is approximately  $5000\text{ W m}^{-1}\text{ K}^{-1}$  [33]. Graphene was suspended, and Young's modulus was characterized by patterning a circular well array having a 1.5 mm diameter and 500 nm depth on a SiO<sub>2</sub>/Si substrate ([Figure 1.2b](#)).

[Figure 1.2c](#) shows the elastic stiffness statistical histogram of suspended graphene. Young's modulus obtained by this method is about 1.0 T Pa [[36](#)]. Therefore, graphene has shown great prospect in applications of electronics, optoelectronics, energy storage, and conversion.

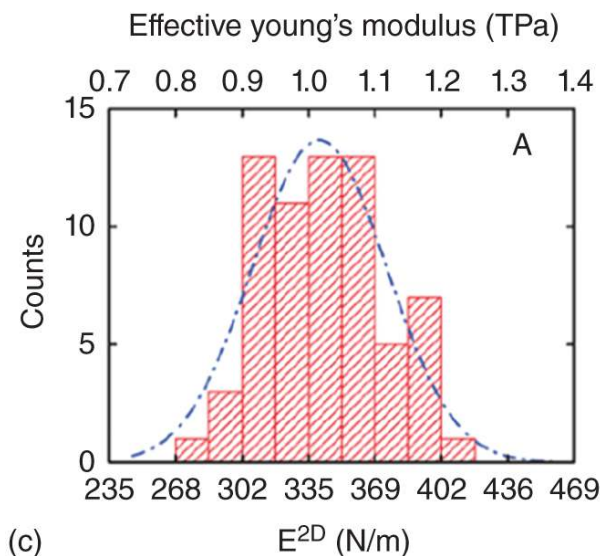
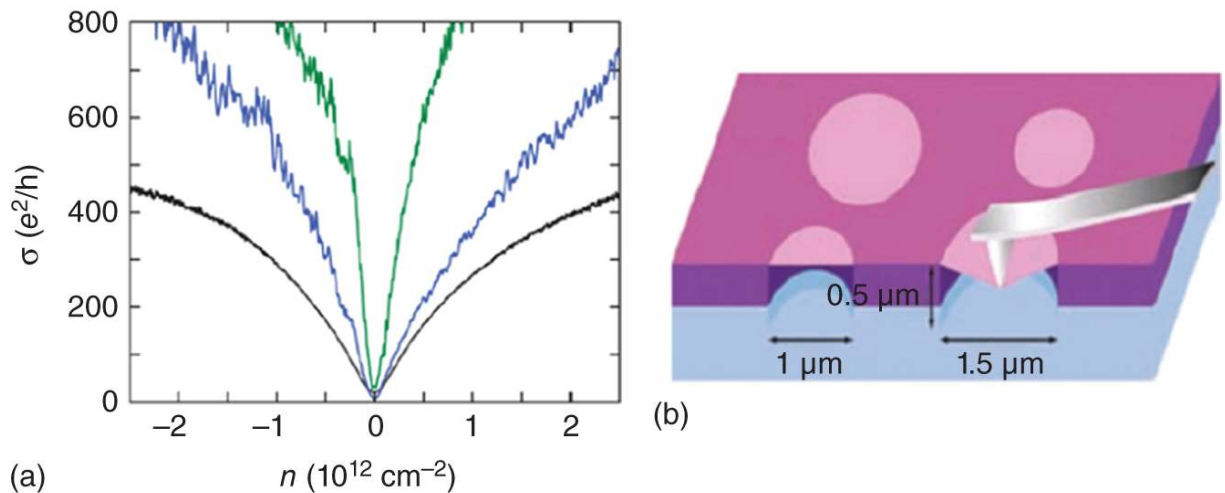


**Figure 1.2** Brief introduction of graphene. (a) Relationship between conductance and density of charge carrier. The black and blue plots were obtained at 300 and 1.6 K, respectively. The green one is consistent with carrier mobility  $\mu = 350\,000\text{ cm}^2\text{ V}^{-1}\text{ s}^{-1}$  from another sample.

*Source:* Reproduced with permission from Ref. [33], © American Chemical Society 2008; (b) schematic of configuration about suspended graphene being indented. (c) Elastic stiffness statistics histogram of graphene.

*Source:* Figure (b) and (c) reproduced with permission from Ref. [34], © Wiley Online Library 2010.

However, graphene still faces significant challenges because of its zero-bandgap nature, which hinders its



eventual application. Another two-dimensional allotrope of carbon breaks the ice. The graphite acetylene and its derivatives composed of  $sp$ - and  $sp^2$ - hybrid carbon atoms have a certain bandgap in the band structure [37-39]. In graphene-acetylene and its derivatives, the alkyne bond is a structural unit that can be inserted to modify the graphene and retain the symmetry of the hexagon. [Figure 1.3a](#) shows the transformation of graphene to  $\alpha$ -,  $\beta$ -, and  $\gamma$ -graphene by inserting acetylene bonds between two carbon atoms in different ways [38]. The structure shown in [Figure 1.3b](#) is formed by graphite diacetylene when two acetylene bonds are inserted [39]. Acetylene chains of different lengths will generate a series of graphitic alkynes, such as graphitic alkynes, graphitic dialkynes, graphitic trialkynes, and graphitic tetrapyne. [41]

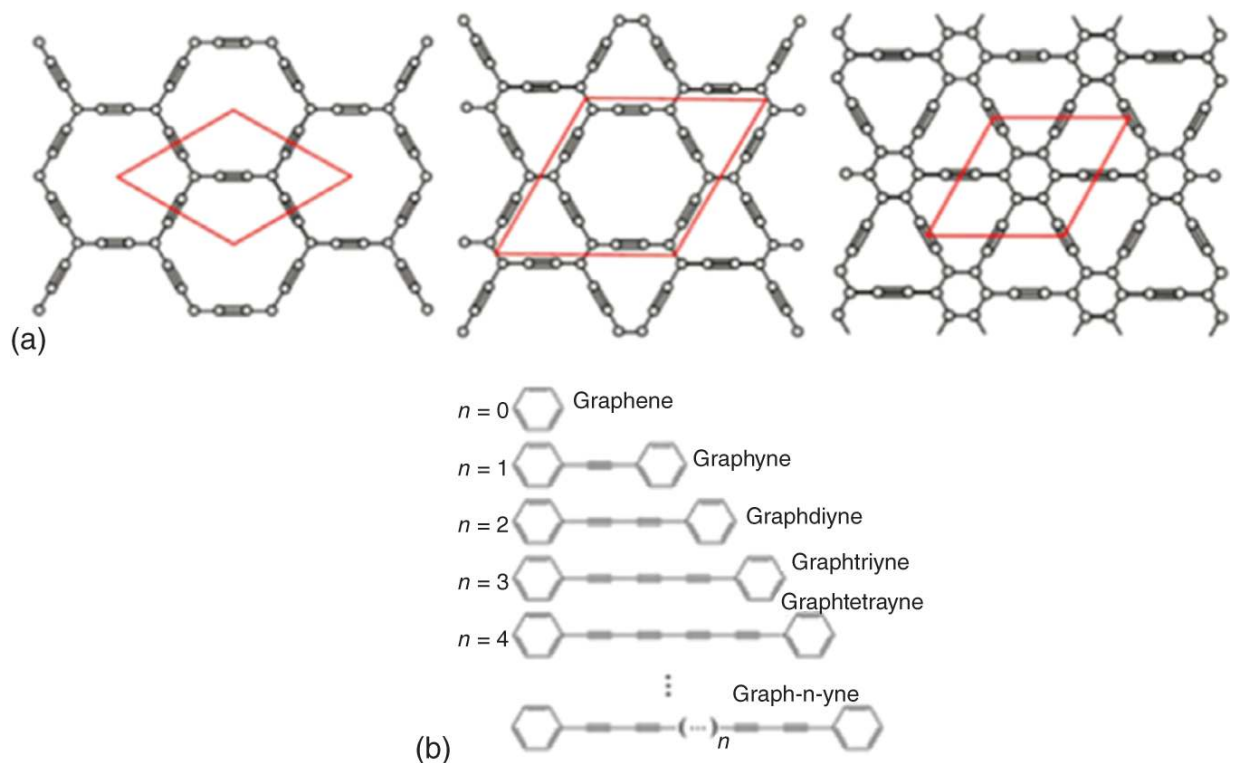


**Figure 1.3** Structure and optoelectronic applications of graphite-acetylene group materials. (a) Structure of alpha-, beta-, and gamma-graphene.

*Source:* Figure (a) reproduced with permission from Ref. [39], © American Chemical Society 2011; (b) expansional diagram of n-alkyne based on chain length.

*Source:* Reproduced with permission from Ref. [40]/ © American Chemical Society 2013.

As one of the graphyne derivatives, graphdiyne can be grown by cross-coupling with hexaethynylbenzene as precursors [40, 42-45]. In general, graphdiyne can be obtained as nanowalls (NWs) [44, 45], film [42, 43], or coating layers covering  $\text{TiO}_2$  [40] by this coupling reaction. In recent years, graphdiyne was successfully prepared on the Au (111) crystal plane using molecular evaporator deposition of precursor molecules in the ultrahigh vacuum ambient of a scanning tunnelling microscopy (STM) [46]. Nishihara et al. successfully prepared multiple layers and few layers of graphite-diacetylene through liquid/liquid or

gas/liquid interface reactions [47]. Its properties are predicted successfully by theoretical calculation. Graphyne allotropes feature an intrinsic bandgap ( $\sim 1.2$  eV for graphyne and  $\sim 0.46$  eV for graphdiyne), and their direct bandgaps indicate their potential applications in optoelectronic devices [48, 49]. Two-dimensional graphene with Dirac dots and cones still exist, such as  $\alpha$ -graphene with a single Dirac cone and 6,6,12-graphene with two different Dirac cones [49, 50]. The different atomic structure of graphyne alkyne results in the difference of electronic structure [51]. Graphyne group material as a new 2DLM has excellent application prospects in electronic devices and photovoltaic devices [40, 43, 49]. Li et al. constructed a solar cell with high efficiency electron transport based on graphite-diacetylene doped benzene-C61-methyl butyrate, as shown in Figure 1.3 [52]. Although graphyne family materials have excellent carrier mobility with a proper bandgap, the challenge of synthesizing single crystal with large scale and high quality has severely limited the further application development of graphite-based alkyne. Wherefore, new methods are urgently needed to achieve the preparation of such high-quality materials.

In addition to carbon, other elements of the IVA group can also form 2DLMs, including silene, germanene, and tinene. The atoms in silicene or germanene are connected with each other through  $sp^3$  hybridization, which is more stable than the  $sp^2$  hybridization. Even if they are not able to exist as independent lamellae, they can still be successfully obtained as layered materials. At present, lots of methods have been reported to grow silene. One of the most effective methods of wet chemistry is the stripping of 2DLMs by an exchangeable Ca layer and an interlinked Si6 ring consisting of  $CaSi_2$  [53]. Some used HCl solution and Mg to further reduce layer-to-layer interactions [54, 55]. In

addition, the most common approach is the vapor deposition on selected substrates, such as Ag (111) [56], Ag (110) [57], Au (110) [58], Ir (111) [59], MoS<sub>2</sub> [60], ZrB<sub>2</sub> [61], and H-MoSi<sub>2</sub> [62] in STM. Excellent physical features of silicene, including the quantum spin Hall effect [63, 64], ferromagnetism [65, 66], germanium doping controlled TC [67], and semi-metallic properties [68] have been predicted by theoretical calculations [69].

Germanene can be prepared in a comparable method as silicene, including CaGe<sub>2</sub>-assisted chemical exfoliation [70] and vapor deposition [71–73]. Germanene features a number of exclusive characteristics, including robust structure [74], semi-metallic property [75], high exciton resonance [76, 77], high carrier mobility [78], Dirac characteristics [79, 80], photon properties of ground state [81, 82], negative thermal expansion [83], spin electron transport [84], tunable magnetism [85], many body effects [86], infrared absorption [87, 88], and great thermoelectric properties [89]. The charge carriers of germanium materials, whose electronic structure is similar to graphene and silicon, are massless fermions. Using a vertical electric field can open the bandgap in a single layer of flexed silicon and germanene [90]. In addition, novel properties of the quantum spin hall effect are able to be realized by halogen or hydrogen elements modification [91, 92].

The Sn (111) diatomic layer where two triangular sublattices are stacked to generate a crooked honeycomb lattice that forms the stanene. Based on the substrate Bi<sub>2</sub>Te<sub>3</sub> (111), stanene can be prepared by molecular beam epitaxy (MBE) [93]. Excellent properties have been predicted through theoretical calculations [94], such as stress-affected mechanical properties, novel thermal transport diffusion properties [95, 96], unique electronic features [97], phase transition between topological phase

to insulating one [98], large magneto-resistive [99], super conductivity [100], and quantum spin Hall effect [101].

### 1.2.2.2 V group A

Two-dimensional materials composed of V-A group elements include black phosphorus (BP), arsenic, antimony, and bismuth. In 1914, BP was successfully prepared [102, 103], where each atom was covalently connected to three adjacent atoms to create a folded monolayer honeycomb. [104] From bulk to monolayer, the bandgap of BP increases (0.3 up to 1.5 eV). In addition, it has been proved that the room temperature carrier mobility of BP in several layers of quasi-2D phosphors is up to  $1000 \text{ cm}^2 \text{ V}^{-1} \text{ s}^{-1}$  [105].

Therefore, BP shows significant prospect in applications of electronic and photonic devices [106]. Current methods for producing BP include mechanical stripping [107–109], liquid stripping, [110–113] and CVD [114]. At the same time, the thickness of BP determines its properties, for example photoluminescence (PL) spectroscopy [109, 110]. BP has been demonstrated to show great potential applications in photoelectric fields [107], including photodetectors and solar cells. [115] BP is studied through simulation experiment and theory analysis of many properties, including stacking-sequence-dependent electronic structure [116–118], anisotropic properties [114], transmission characteristics between magneto-optical [119], controlled band structure [120, 121], flexibility [122], thermal properties [123], anisotropic exciton [124], and electrical conductance [125]. Interestingly, blue phase [126, 127] and topological insulator conversion of BP are proved [128].

Structurally, a layer of arsenic atoms with a rhombic structure forms arsenic. Thickness of 14 nm arsenic was successfully grown on InAs substrate via plasma-assisted process [129]. It has been theoretically calculated that

arsenic has many exclusive characteristics, covering anisotropic-controlled TC [130] and strain-modulated topological insulator conversion [131].

The most stable V-A group allotropes is antimonene with monolayer antimony. The bandgap is predicted as 2.28 eV. At present, the approaches of preparing antimonene are mainly mechanical stripping [132], liquid exfoliation [133], MBE [134], and CVD [135]. Antimonene is predicted theoretically to feature some novel characteristics, including spin-orbit coupling (SOC) effect [136], geometry-controlled TC [137], defects-controlled electronic properties [138], and UV detection [139]. Indirect to direct bandgap transition would occur through a small stress, further advancing its potential in optoelectronic applications [140, 141].

In 2005, bismuth was first grown on atomically smooth surfaces [142]. After that, bismuth was successfully obtained by wet chemical synthesis [143]. Theoretical calculations show that bismuthene has a lot of nice attributes. At high temperature, bismuth is insensitive to long wavelength vibration and thermal excitation. As the 3D bulk is scaled into individual single-layer sheets, the bismuthene's structure is compressed, resulting in a transformation from a semi-metal to a semiconductor. Nevertheless, such thickness dependence does not affect the topological characteristics of bismuthene [144, 145].

### **1.2.2.3 III A Group**

In Group III A, the last specific elemental 2DM is borophene. Boustani first proposed the quasi-planar boron structures through theoretical calculations [146]. Later, methods for preparing borophene, such as vapor deposition [147, 148] and two-growth-zone CVD, were reported [149]. More simulations show that borophene has lots of special